Magnetic Structures of MnO, FeO, CoO, and NiO†

W. L. ROTH

General Electric Research Laboratory, Schenectady, New York

(Received February 28, 1958)

The antiferromagnetic arrangement of moments in MnO, FeO, CoO, and NiO have been investigated by powder neutron diffraction. The results for the four oxides are consistent with a structure in which the magnetic moments are arrayed in ferromagnetic sheets parallel to (111) planes, and the direction of magnetization in neighboring planes is antiparallel. The observation of diffuse neutron scattering limits the precision with which the magnetization direction can be specified. If the diffuse intensity is included with the Bragg scattering, the direction of magnetization in MnO, and NiO lies within the (111) plane; for CoO, the preferred direction is [$\bar{1}\bar{1}7$], intermediate to the (111) plane and the tetragonal axis. The magnetic axis in FeO is perpendicular to the ferromagnetic sheet.

INTRODUCTION

IN their classic paper on the scattering of neutrons by paramagnetic and antiferromagnetic solids, Shull, Strauser, and Wollan described the arrangement of the atomic spins in the antiferromagnetic state of MnO, FeO, CoO, and NiO.[1] The analysis is of considerable significance because it is direct experimental verification of the Néel hypothesis of an ordered antiferromagnetic arrangement of atomic spins and the superexchange interaction postulated by Kramers.[2] The crystal structure of all the monoxides is of the NaCl type, and the reported magnetic structure consists of (111) sheets of magnetic atoms in which the spins are parallel, but with an alternation of spin direction in adjacent sheets. The spin direction in MnO, CoO, and NiO was reported to be parallel to [100], and in FeO parallel to [111].

We have re-examined these magnetic structures in order to resolve the relationship between the antiferromagnetic arrangement of spins and the crystal distortions which occur when the oxides pass from the paramagnetic to the antiferromagnetic state. In the paramagnetic state, the symmetry of all the oxides is cubic; in the antiferromagnetic state there is a small crystallographic distortion.[3,4] MnO and NiO become rhombohedral with $\alpha > 60°$, FeO becomes rhombohedral but with $\alpha < 60°$, whereas CoO becomes tetragonal with $c/a < 1$. However, Shull and co-workers concluded that the spin structures of MnO, CoO, and NiO were identical, and only in the case of FeO does the spin structure conform with the crystal symmetry.

The theory of antiferromagnetism has recently been reviewed by Nagamiya, Yosida, and Kubo,[5] and the most recent calculations of the anisotropy energies of the *M*O oxides have been made by Kanamori.[6] Two mechanisms for the deformation below the Néel

temperature can be distinguished: one is magneto-striction which arises from anisotropy energies and depends on the orientation of the magnetic moments; another is "exchange-striction" which arises from the dependence of the exchange energies on interionic distances. Greenwald and Smart[7,8] have discussed the crystallographic deformations as a consequence of the exchange interactions, and Shull *et al.* base their analysis of the neutron diffraction pattern of MnO on a similar premise. On the other hand, Li[9] has proposed an alternative set of antiferromagnetic structures and considers the deformations a consequence of anisotropy magnetostriction.

The anisotropy energies of FeO and CoO have been computed by Kanamori. The orbital state is degenerate and the magnetic anisotropy is considered to originate from four sources: (1) magnetic dipole-dipole inter-actions, (2) spin-orbit interactions, (3) orbit-orbit interactions, (4) anisotropy energy arising from de-formation. The calculations suggest that the principal source of magnetic anisotropy energy in the deforma-tion-free state originates from orbital multipole inter-actions, but the deformation of the crystals is a consequence of magnetostriction arising from the crystalline field energy dependent on deformation. It is concluded that in CoO the magnetization should be in the direction of the tetragonal axis, whereas in FeO the magnetization should be along the trigonal axis. In MnO and NiO the orbital state is nondegenerate, the dipole-dipole interaction predominates, and the magnetization should lie within the (111) plane. This is contrary to the conclusions of Li who predicts the spin direction in MnO and NiO to be perpendicular to the (111) plane. The various magnetization directions are summarized in Table I.

ANTIFERROMAGNETIC MOTIFS AND THE MAGNETIC RECIPROCAL LATTICE

The problem is best formulated in terms of the scattering of neutrons by a single-domain single crystal;

† Experimental work carried out at the Brookhaven National Laboratory Reactor, Upton, New York.

[1] Shull, Strauser, and Wollan, Phys. Rev. **83**, 333 (1951).

[2] H. A. Kramers, Physica **1**, 182 (1934).

[3] H. P. Rooksby, Acta Cryst. **1**, 226 (1948).

[4] N. C. Tombs and H. P. Rooksby, Nature **165**, 442 (1950).

[5] Nagamiya, Yosida, and Kubo, *Advances in Physics* (Taylor and Francis, Ltd., London, 1955), Vol. 4, p. 1.

[6] J. Kanamori, Progr. Theoret. Phys. (Japan) **17**, 177 (1957); **17**, 223 (1957).

[7] S. Greenwald and J. S. Smart, Nature **166**, 523 (1950).

[8] S. Greenwald and J. S. Smart, Phys. Rev. **82**, 113 (1951).
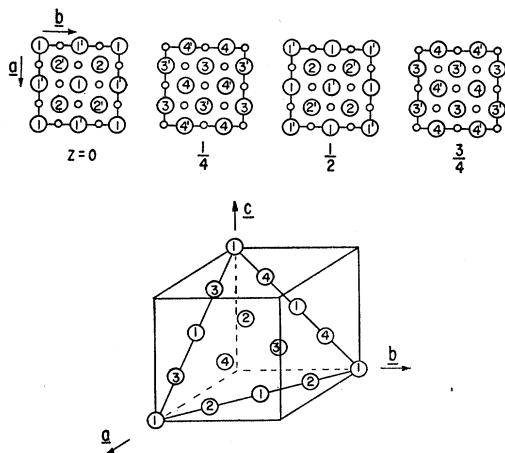
[9] Y. Y. Li, Phys. Rev. **100**, 627 (1955).

FIG. 1. The magnetic unit cell. The 32 atomic moments are distributed among 8 magnetic sublattices, paired to generate 4 antiferromagnetic submotifs.

powder diffraction intensities in the form $\{hkl\}$ then are computed by summing the single-crystal intensities (hkl). The crystallographic distortions are small and it is convenient to use pseudocubic unit cells to describe the crystals in the antiferromagnetic state.

In the paramagnetic state the four oxides crystallize in the cubic NaCl arrangement. In the antiferromagnetic state magnetic scattering is observed which requires that the unit cell edge be doubled; the pseudocubic magnetic cell contains 32 magnetic ions. The doubling of the unit cell requires alternate metal ions parallel to the unit translations to differ in a magnetic sense. Designating the difference by primes, the magnetic ions are distributed as shown in Fig. 1. The magnetic ions fall into four submotifs,* each containing eight ions. The primed ions must be magnetically distinguishable from the unprimed ions in the same submotif, but are not necessarily antiparallel. The doubling of the magnetic unit cell edge does not require any relationship between the spins on differing submotifs. The magnetic structure problem then is to discover the structure of each submotif (the spin directions of the two distinguishable magnetic ions) and the relationship of the submotifs to each other.

The problem is greatly simplified if two assumptions are made: (a) the direction of alternate spins in each submotif is antiparallel, in accordance with the usual superexchange hypothesis; (b) there is a single magnetic axis in the unit cell, i.e., in an antiferromagnetic domain the spin directions in all submotifs are parallel and antiparallel to a single crystallographic direction. Solutions to the magnetic structures first will be found with the assistance of these two restrictive assumptions; the consequences of discarding assumption (b) will be

* The term submotif is preferred to sublattice since the points are not translation equivalent. An alternative designation is substructure, but this would lead to confusion with magnetic domains.

considered in a following paper on multispin axis structures.

There are only two ways in which the four magnetic submotifs may be correlated in a single magnetic axis structure. These are shown as A and B in Fig. 2, where the designations are the same as those given by Li. For the magnetic cell which contains 32 MO, we find for the nuclear and magnetic structure factors:

Models A and B:

$$F_{nucl} = 32 \ (f_M + f_O) \ \text{if} \ h+k+l=4n$$
$$= 32 \ (f_M - f_O) \ \text{if} \ h+k+l=4n+2$$
$$= 0 \qquad \text{if} \ h+k+l=4n\pm1. \qquad (1)$$

Model A:

$$F_{mag} = 32 \ p_M \qquad \text{if} \ h, k, l \ \text{are all odd and}$$
$$h+k, \ k+l, \ l+h=4n+2$$
$$= 0 \qquad \text{otherwise.} \qquad (2)$$

Model B:

$$F_{mag} = 16 \ p_M \qquad \text{if} \ h, k, l \ \text{are all odd}$$
$$= 0 \qquad \text{otherwise.} \qquad (3)$$

In these equations, f_M and f_O are the nuclear scattering amplitudes of the M and O nuclei, and p_M is the magnetic scattering amplitude which depends on both the magnetic moment of the M ion and the magnetic form factor. The scattering of an unpolarized neutron beam by both nuclei and oriented atomic spins is given by

$$F^2 = F_{nucl}{}^2 + q^2 F_{mag}{}^2, \qquad (4)$$

$$q^2 = 1 - (e \cdot k)^2 = \sin^2\alpha, \qquad (5)$$

where α is the angle between the unit vectors e and k parallel to the scattering and magnetic vectors, respectively.

In a single crystal the nuclear and magnetic scattering are completely resolved, the nuclear scattering being confined to reciprocal lattice points making up the forms $\{222\}$, $\{400\}$, $\cdots$ and the magnetic scattering to the forms $\{111\}$, $\{113\}$, $\{333\}$, $\cdots$. The magnetic reciprocal lattice of the two antiferromagnetic arrangements A and B is quite different. For model A there are magnetic space group absences for which the value

TABLE I. Magnetic axes and crystal deformations in antiferromagnets. The symbol (hkl) means the spin lies within the plane hkl and the direction is not further specified; $[UVW]$ refers to the specific crystal direction.

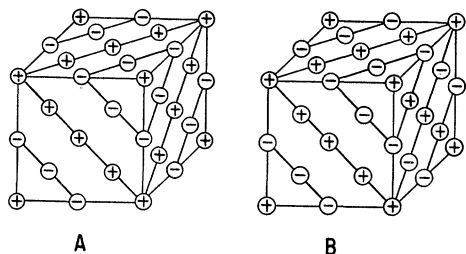| Compound	MnO	FeO	CoO	NiO
Néel temp. °K	122	198	291	523
Symmetry	Rhomb.	Rhomb.	Tetr.	Rhomb.
	$\alpha<60°$	$\alpha>60°$	$c/a<1$	$\alpha<60°$
Magnetization				
Shull et al.	[001]	[111]	[001]	[001]
Li	[111]	[111]	[001]	[111]
Kanamori	(111)	[111]	[001]	(111)

FIG. 2. Correlation of magnetic sublattices. These are the two possible correlations subject to the restriction that there is a single magnetic axis within the cell.

of F^2 vanishes regardless of the direction of the atomic spins. Thus in the form {111} only two reflections, (111) and ($\overline{1}11$), are possible whereas the remaining six must be identically zero. On the other hand, in model B the structure factor F^2 is the same for all members of the form {111} and the intensities of the individual reflections are determined only by q^2.

There is an unfortunate ambiguity when the problem is considered from the point of view of powder diffraction. The powder diffraction peak {hkl} is a composite of the individual reflections (hkl). From Eq. (2) it may be seen that the spin arrangement in model A gives rise to absences which have the effect of reducing the usual multiplicity factor J by $\frac{1}{4}$. For the spin structure described by Shull for MnO, CoO, and NiO, which corresponds to model A with the spins pointing along a cube edge, the magnetic intensities are given by $\frac{1}{4}J(32p_M)^2(q^2)_{Av}$, where $(q^2)_{Av} = \frac{2}{3}$ for all the magnetic peaks. In model B the multiplicities are not reduced, but the magnetic intensities are given by $J(16p_M)^2(q^2)_{Av}$, and $(q^2)_{Av} = \frac{2}{3}$ for any direction of the magnetic spins. Consequently, powder diffraction information is unable to distinguish between the Shull structure $A_{[001]}$ and structures based on model B with any spin direction. It was this observation that lead Li to suggest the alternative structures based on B but with various spin directions which would be consistent with the crystallographic distortions.

NEUTRON DIFFRACTION POWDER PATTERNS

Neutron diffraction patterns have been obtained from powders of MnO, FeO, CoO, and NiO at temperatures down to 4.2°K. Monochromatic neutrons with $\lambda = 1.02$ A were selected from the pile spectrum by diffraction from a lead monochromator crystal, collimated by Soller slits, and detected by a BF_3 counter. The counting times were determined by a monitor in the incident beam, and the usual pattern was measured at angular intervals of about 0.1°, counted for approximately 25 minutes at each point. The observed integrated intensities are compared with those computed from F_{calc}^2 after applying the appropriate normalization, angular, absorption, and temperature factors.

SAMPLE PREPARATION

We are grateful to Dr. Ralph Carter of this laboratory for preparing the samples of MnO, FeO, and CoO. The MnO was produced by heating Johnson, Matthey Mn_3O_4 at 1100°C in dry hydrogen for 24 hours, and quenching. The CoO was prepared from Johnson, Matthey Co_3O_4 by heating to 1300°C in air and quenching. Since FeO exists over a large range of composition, particular care was taken to prepare specimens in such a manner that the composition would be known. The raw material was Johnson, Matthey Fe_2O_3 and 10-gram specimens were equilibrated at 1100°C in water-hydrogen atmospheres in accordance with the equilibrium data of Darken and Gurry.[10] The composition of each FeO lot was checked by x-ray diffraction and the individual lots combined to obtain the large sample required for neutron diffraction. Magnetic measurements proved the absence of a ferromagnetic phase. The NiO was a special sample provided by the Merck Chemical Company.

MnO

The neutron diffraction pattern obtained from MnO at 4.2°K is shown in Fig. 3. Magnetic superstructure peaks are observed which confirm the observation by Shull that the magnetic unit cell edge is double that of the nuclear cell. One essential difference in the patterns stems from the present use of higher resolution so that the magnetic {113} and nuclear {222} peaks are resolved. The aluminum scattering from the specimen holder and cryostat do not interfere with the MnO pattern.

Careful inspection of the data reveals that the background level beneath {111} is abnormal; there is a small but significant diffuse intensity ranging from approximately 9° to 15°. Several experiments were carried out to confirm the reality of the diffuse scatter-
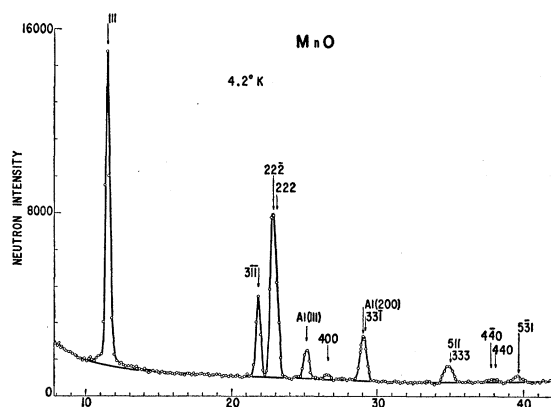

FIG. 3. Neutron diffraction pattern from MnO at 4.2°K. The asymmetry of {222} is a consequence of the rhombohedral deformation.

[10] L. S. Darken and R. W. Gurry, J. Am. Chem. Soc. 68, 798 (1946).

ing. A diffraction pattern was obtained in which a cadmium shutter was periodically inserted so as to intercept the diffracted beam just before it entered the BF_3 counter. In this way a measure of the instrumental and environmental background was obtained and the presence of diffuse scattered intensity confirmed. Further confirmation was provided by L. Corliss and J. M. Hastings of Brookhaven National Laboratory who kindly prepared a diffraction pattern of our material using their apparatus and obtained a comparable result.

The diffuse neutron intensity introduces a complication into the interpretation of the diffraction pattern. It is not clear at this time whether the diffuse scattering should be included in the integrated intensity of the {111} Bragg peak. Broadly speaking, there are two likely origins of the diffuse scattering. First, the scattering may be predominantly inelastic in that there is significant momentum and energy transfer between the scattered neutron and the crystal. In this case the diffuse scattering should not be included in the Bragg peak which is to be interpreted as the consequence of the scattering of neutrons by the periodic spin lattice of the crystal. The second source of diffuse intensity is scattering which is not concentrated in the Bragg peak because the scattering system fails to meet the requirements of three-dimensional periodicity. If the diffuse scattering is magnetic in origin, it could arise from the scattering of neutrons by spins in domain boundaries, from short-wavelength spin waves, or magnetic faulting. For these cases the physically significant solution is that in which the diffuse scattering is included in the Bragg peak and the resultant analysis corresponds to a description of the spin system in a perfect single-domain crystallite. The latter analysis is analogous to the thermal diffuse scattering of x-rays.

In Table II are summarized the observed integrated neutron intensities and intensities calculated from several spin models subject to the limitations of super-
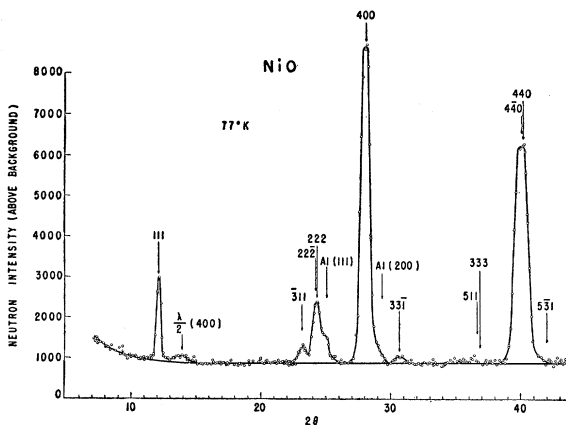
exchange and a single magnetic axis common to the submotifs. Since the Mn^{+2} ion is in a spectroscopic $S_{\frac{5}{2}}$ state, its magnetic moment is due to spin only ($\mu = 5\mu_B$) and the magnetic scattering amplitude is $p = (e^2\gamma/mc^2)Sf$ $= 0.539\times10^{-12}(\frac{5}{2})f$, where f is the magnetic form factor. The intensity scale was established by normalizing with respect to the nuclear peaks.

The first column gives the intensities computed for the structures $A_{[001]}$ or $B_{[UVW]}$, corresponding to the structure originally proposed by Shull and the alternative suggested by Li. Both models predict too small an intensity for {111}, even after the diffuse intensity is subtracted from the Bragg peak. A sensitive criterion for the agreement of models is the intensity ratio {111}/{113} since the ratio is independent of normalization errors. The predicted ratio for $A_{[001]}$ is 2.0, whereas the observed ratio is 3.1 or 3.9 depending on the inclusion of the diffuse scattering.

The remainder of the models must be based on the A structure, a structure in which the spins are ferromagnetically arrayed in planes parallel to (111).

TABLE II. Neutron diffraction intensities for MnO at 4.2°K.

{hkl}	$A_{[001]}, B_{[UVW]}$	Spin arrangement					Observed[a]
		$A_{(111)}$	$A_{[2\bar{1}\bar{1}]}$	$A_{[11\bar{1}]}$	$A_{[\bar{3}\bar{2}\bar{1}]}$	$A_{[22\bar{3}]}$	
111	673	1009	785	897	913	989	804 (1002)[b]
113	331	256	306	280	227	401	258
222	665	665	665	665	665	665	665
400	17	17	17	17	17	17	20
331	105	113	107	110	110	112	110
333,115	56	71	61	66	67	44	88
440	18	18	18	18	18	18	22
531	36	36	32	26	26	36	44

[a] Cylindrical specimen 2-cm diam; $f_{Mn} = -0.37\times10^{-12}$ cm, $f_O = 0.58\times10^{-12}$ cm; $p = 1.35\times10^{-12} f_{mag}$; $2B = 1.0\times10^{-16}$ cm².
[b] Includes diffuse scattering.

Several models exhibiting approximate agreement are given in Table II. The best agreement is found for $A_{(111)}$, the structure where the spin direction lies within the ferromagnetically coupled (111) sheet. The powder data does not discriminate between directions within (111), so various directions $[\bar{1}10]$, $[11\bar{2}]\cdots$ are possible. This agreement is obtained if the diffuse scattering is included in the Bragg peak and suggests that the origin of diffuse intensity is in the disorganization of the spin structure. If the diffuse scattering is not included, to obtain agreement it is necessary to tip the spins out of the (111) plane. Since the minimum value for the ratio {111}/{113} is greater than 3, the best agreement is obtained for model $A_{[11\bar{1}]}$ in which the spins point along a cube body diagonal [but not that diagonal which is normal to the ferromagnetic (111) sheet].

The low-temperature neutron diffraction data confirm the previously reported x-ray studies which showed that the antiferromagnetic form of MnO is rhombohedral, and provide in addition an estimate of the

FIG. 4. Neutron diffraction pattern from NiO at 77°K. Rhombohedral indices are used to describe the crystal deformation.

magnitude of the distortion. As a consequence of rhombohedral distortion, the nuclear {222} peak should split into two components and the {400} peak should remain single. Large-scale plots show that this indeed is the case, and from the asymmetry of the {222} {22$\bar{2}$} peak one estimates for the magnetic cell of MnO at 4.2°K.

$$a_0 = 8.873 \text{ A}, \quad \alpha = 90°26.$$

Utilizing these parameters, the angular positions of the magnetic peaks of the distorted cell have been computed. The magnetic scattering appears to be concentrated in {11$\bar{1}$}, and no scattering is observed at {111}, in agreement with the conclusion that the structure is based on ferromagnetic sheets perpendicular to the rhombohedral axis.

NiO

Neutron diffraction patterns from powders of NiO were obtained at room temperature and at 77°K

TABLE III. Neutron diffraction intensities for NiO at 77°K.

hkl	Spin arrangement			Observed[a]
	$A_{[100]}, B_{[UVW]}$	$A_{[11\bar{1}]}$	$A_{(111)}$	
111	246	328	369	326[b]
113	126	107	98	97
222	309	309	309	327
400	2212	2212	2212	2207
331	48	51	52	49
333,115	30	36	39	38
440	2168	2168	2168	2178
531	26	22	30	89[c]
335,226	247	245	245	290
444	938	938	938	943

[a] Intensities are averaged from four traverses; cylindrical specimen 2-cm diam; $f_{Ni} = 1.03 \times 10^{-12}$ cm, $f_O = 0.58 \times 10^{-12}$ cm; $p = 0.539 \times 10^{-12}$ f_{mag}; $2B = 1.0 \times 10^{-16}$ cm².
[b] No allowance for diffuse scattering included in this value.
[c] Includes Al(220) from cryostat.

(Fig. 4). The results are qualitatively similar to those observed for MnO, although the visual appearance of the patterns is considerably altered as a consequence of the negative nuclear scattering amplitude of Mn which reverses the relative intensities of the nuclear peaks. There is a magnetic superstructure which can be indexed on a magnetic cell with $a_{mag} = 2a_{nucl}$, and again there appears to be diffuse neutron scattering in the vicinity of the magnetic {111} peak. Although the spectroscopic state of the free Ni^{+2} ion is $^3F_4$, the crystalline field should quench the orbital contribution to the magnetic moment and the resultant should be essentially $2\mu_B$, the spin-only value.[11] Since the crystallographic distortions of MnO and NiO in the antiferromagnetic state are both rhombohedral with $\alpha > 90°$, the antiferromagnetic structures are expected to be similar.

---

[11] See, for example, J. H. Van Vleck, *Electric and Magnetic Susceptibilities* (Oxford University Press, New York, 1932), pp. 282–310.
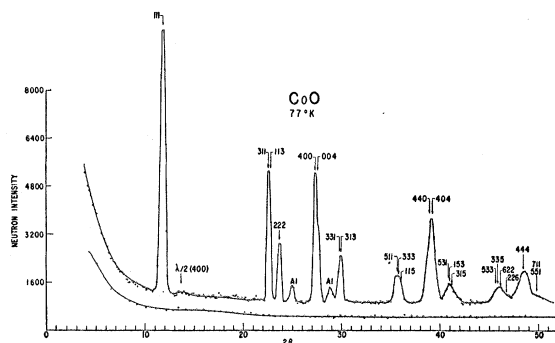

FIG. 5. Neutron diffraction pattern from CoO at 77°K. The asymmetry of {400} and {440} is a consequence of the tetragonal deformation.

These conclusions are confirmed by the neutron diffraction data summarized in Table III. The observed intensity ratio {111}/{113} = 3.4 again serves to eliminate the original structure $A_{[100]}$ or the group of structures $B_{[UVW]}$ which requires a ratio of 2.0. Reasonable agreement between observed and calculated intensities is obtained for model $A_{(111)}$, the structure in which the spins lie in an unspecified direction in the ferromagnetically coupled (111) sheet; as with MnO, this agreement would be improved by including diffuse scattering in the Bragg peak. To obtain quantitative agreement approximately 12% of the intensity would be associated with diffuse scattering, as compared with 20% for MnO. The positive identification of diffuse scattering is more difficult in this case since the magnetic scattering is much smaller and there is interference from the relatively strong $\frac{1}{2}\lambda$ component of {400}. The intensity in the region of 14° appears too large to be completely accounted for by $\frac{1}{2}\lambda$, and it is possible to account for the discrepancy, $I_{calc} - I_{obs} \simeq 43$, by diffuse scattering in the vicinity 13°–15°. On the other hand, if allowance is not made for diffuse scattering, the spins must be tipped out of the (111) sheet and intensities computed for the structure $A_{[11\bar{1}]}$ again are in satisfactory agreement with the observations.

The room-temperature results agree with those obtained at low temperature if the room-temperature moment of Ni^{+2} is taken as 1.9 Bohr magnetons, in agreement with the value computed assuming a Brillouin curve with $J = \frac{1}{2}$. The temperature factor $B = 0.5 \times 10^{-16}$ cm², obtained from the nuclear scattering, yields $\theta_D \simeq 490°K$ in fair agreement with low-temperature specific heat data.[12]

CoO

The neutron diffraction patterns obtained from powder samples of CoO at 77°K and 4.2°K (Fig. 5) are qualitatively similar to those observed for MnO and NiO. The quantitative analysis of the magnetic

---

[12] R. R. Wenner, *Thermochemical Calculations* (McGraw-Hill Book Company, Inc., New York, 1941), p. 145.

TABLE IV. Neutron diffraction intensities for
CoO at 77°K and 4.2°K.

| | Nuclear scattering. {400} = 1000 | | | | | | |
| | | | $f_{Co} \times 10^{12}$ | | | | |
{hkl}	0.29	0.28	0.27	0.26	0.25	0.24	Observed[a]
222	198	217	238	259	282	307	290
400	1000	1000	1000	1000	1000	1000	1000
440	972	972	972	972	972	972	972
226	153	168	184	200	217	236	211
444	422	422	422	422	422	422	<522

| | Magnetic[b] scattering. {111} = 1000 | | | | | |
| | | | Spin arrangement | | | |
{hkl}	$A_{(111)}$	$A_{[\bar{1}\bar{1}1]}$	$A_{[\bar{1}\bar{1}7]}$	$A_{[10°]}$	$A_{[001]}$	Observed[a]
111	1000	1000	1000	1000	1000	1000
113	253	312	345	376	491	344
331	130	142	150	156	181	163
333,115	93	97	99	121	109	149
531	66	55	61	...	85	129
335	13	16	18	...	25	17
117,551	23	25	26	...	31	<82
∡ [UVW],[001]	55°–90°	35°	11½°	10°	0°	

[a] Cylindrical specimen 2-cm diam; $f_0 = 0.58 \times 10^{-12}$ cm; $2B = 1.0 \times 10^{-16}$ cm².
[b] To relate nuclear and magnetic intensity scales: $I_{\{111\}}/I_{\{400\}} = 1.91$.

scattering is not as straightforward, however, since the Co^{+2} ion is in a $^4F_{9/2}$ state and a partial contribution of the orbital moment to the total magnetic moment is expected.[11] Consequently, whereas for MnO the only adjustable parameters are those related to the arrangement and orientation of spins, for CoO the magnitude of the magnetic scattering amplitude must also be deduced from the diffraction data. An additional complication is that because of the extremely large tetragonal deformation (there is a 1.2% contraction along the c axis in the magnetically ordered state), it is probable that the 3d electron radial distribution function about the Co^{+2} ion deviates considerably from a spherical distribution, and consequently the magnetic scattering amplitude will be asymmetric.

Our earlier results led to the conclusion that the moments in antiferromagnetic Co O were ordered according to the A structure, but that the moment direction must be tipped out of the ferromagnetic (111) sheet, and the most probable spin direction was approximately along [111].[13] Since this result was unexpected and suggested that the magnetic arrangement was a compromise between the magnetic dipole forces which tended to order the moments within the (111) plane and the crystal anisotropy which tended to orient them parallel to [001], the measurements were repeated with improved experimental conditions. The present results agree with those obtained previously, but because of the improved statistical precision, there now are observed significant discrepancies between observed and calculated intensities. The present data require a revision of the value of the coherent nuclear scattering

cross section of cobalt, and since the cobalt cross section in turn enters into the determination of the value of magnetic moment of Co^{+2}, it is desirable for clarity to consider the nuclear and magnetic scattering separately.

The integrated intensities for the nuclear peaks are given in Table IV on the basis of an arbitrary scale where the intensity of {400} = 1000. The {222}, {400}, and {440} peaks are clearly resolved, but {226} and {444} have been reduced by subtracting the calculated magnetic contribution. If one uses the accepted value for the nuclear scattering amplitude of cobalt (0.28 $\times 10^{-12}$), the relative intensities of {400}/{222} should be 1000/217, whereas the observed ratio is 1000/290. Since this discrepancy is of the same order as the differences in intensities expected for the various magnetic structures, several additional experiments were undertaken to increase our confidence in the reliability of the results.

CoO is thermodynamically unstable with respect to Co_3O_4 at room temperature, so the crystallographic and chemical integrity of the sample was rechecked by x-ray and chemical analysis. X-ray diffraction patterns showed only the expected lines for CoO, and chemical analysis for cobalt gave the following results: found,[14] $(78.6 \pm 0.15)\%$; calculated for CoO, 78.65%. The specimen was single-phase and stoichiometric.

The possibility that the anomalous intensities were due to preferred orientation and/or extinction was eliminated by obtaining similar results from the specimen after regrinding and lightly packing in a flat glass holder (in place of the aluminum cylindrical holder used for the low-temperature experiments). The significant angular region was shown to possess no abnormal fluctuations in background intensity, and the linearity of our neutron detection system was checked by attenuation experiments. The possibility that the anomalous intensities were due to atomic displacements in the low-temperature tetragonal modification was eliminated by room-temperature experiments, which showed that the same intensity ratio was observed in the cubic phase.

The observed nuclear intensities are easily accounted for by reducing the value for the coherent scattering amplitude of cobalt from 0.28×10^{-12} to 0.25×10^{-12} cm (corresponding to a reduction in cross section from 0.98×10^{-24} to 0.78×10^{-24} cm²). In Table IV are given the computed intensities for several values of f_{Co}. The observed value for {444} is uncertain since it depends on an extrapolation of the measurements to large angles, as well as correction for contributions from {117} and {551}.

The magnetic scattering from CoO in the magnetically ordered state is summarized in Table IV. Identical results were obtained at 77°K and 4.2°K,

[13] Magnetic arrangements of MnO, FeO, CoO, and NiO. Presented at Neutron Diffraction Symposium, American Crystallographic Association, French Lick Meeting, June, 1956.

and the tabulated data are the average of runs at both temperatures. Comparison of the relative intensities with those computed for several models clearly show the data are inconsistent with a structure in which the moments lie along the tetragonal c axis ($A_{[001]}$) or one in which the moments lie in the (111) plane. In the final row are given the angles the magnetic axes make with the tetragonal c axis. Reasonable agreement is obtained if the moment direction is taken between the two extremes: $A_{[\bar{1}\bar{1}1]}$ is satisfactory, but the agreement is further improved if the moment direction is taken parallel to $[\bar{1}\bar{1}7]$, a direction which makes an angle of $11°30'$ with respect to $[001]$. The intensities at large angles are somewhat greater than computed, suggesting that $f_{Co^{+2}}$ does not decrease as rapidly with $\sin\theta/\lambda$ as was assumed by scaling with respect to $f_{Mn^{+2}}$.

The original theory of Kanamori predicted the magnetization of CoO should be along {001}, with a possible 2° deviation from the tetragonal axis. Nagamiya and Matizuki[15] have modified the theory and conclude that the magnetic axis in CoO might deviate as much as 10° from the c axis of the tetragonal cell. The column headed $A_{[10°]}$ gives the results of their calculations for the A model in which the axis is tilted 10° away from $[001]$. Their model essentially is identical with $A_{[\bar{1}\bar{1}7]}$, and the difference in calculated intensities reflects the effect of the asymmetric magnetic form factor since Nagamiya and Matizuki have utilized the wave functions deduced by Kanamori for CoO.

The shapes of the nuclear peaks are in agreement with the x-ray observation that the symmetry of the low-temperature antiferromagnetic state of CoO is tetragonal. The tetragonal deformation results in the splitting of the {400} and {440} peaks into two components, whereas the {222} peak remains single. The peaks in Fig. 5 clearly show this deformation, and the separation of {400} from {004} (somewhat exaggerated in drawing) agrees both in magnitude and intensity with the previously reported compression of the cell corresponding to $c/a = 0.988$.

As a consequence of the large tetragonal distortion it is possible to obtain from the powder pattern additional information about the spin directions in CoO. In the

FIG. 6. Neutron diffraction pattern from FeO at 4.2°K.

tetragonal cell, the magnetic reflections {11$\bar{3}$} and {$\bar{3}$11} are not equivalent, although both are allowed by the A motif and have nonvanishing values for F_{mag}^2. Accordingly, the relative intensities of {11$\bar{3}$} and {$\bar{3}$11}, and similarly {33$\bar{1}$} and {$\bar{1}$33}, depend on the direction of the magnetic moment. From Fig. 5 it is apparent that $I_{\{\bar{3}11\}} > I_{\{11\bar{3}\}}$ and also $I_{\{33\bar{1}\}} < I_{\{\bar{1}33\}}$. In Table V are summarized the intensities computed for several models $A_{[UVW]}$, and it is clear that the only acceptable structures are those in which the magnetic moment has an appreciable component parallel to the tetragonal axis.

The absolute values for the magnetic intensities depend on the magnetic moment of the Co^{+2} ion. The experimental ratio of the magnetic to nuclear scattering gives $3.80\mu_B$ for the magnetic moment of Co^{+2}. From paramagnetic susceptibility measurements on CoO·MgO solid solutions, Elliott has reported $P_{eff} = 5.1$,[16] corresponding to a moment $4.2\mu_B$, 10% larger than the present value deduced by neutron diffraction.

FeO

The final member of the antiferromagnetic series, FeO, differs from the others in that the compound exists over a broad range of composition. The relationship between the magnetic interactions and the nonstoichiometry will be reported separately, and it is sufficient to consider here only the general nature of the antiferromagnetic structure and its bearing on those of the other MO compounds.

The symmetry of the deformation of the low-temperature form is rhombohedral, but contrary to MnO and NiO, $\alpha < 90°$ and the cell is elongated along the $[111]$ axis. Neutron diffraction patterns were obtained at room temperature and 4.2°K (Fig. 6), and in agreement with Shull *et al.* the magnetic {111} superstructure peak is absent, except for some diffuse non-Bragg scattering. The absence of {111} immediately eliminates all models based on A or B except for $A_{[111]}$, the structure based on ferromagnetic sheets parallel to

TABLE V. Resolution of spin direction with respect to tetragonal axis of CoO. Neutron intensities computed for $A_{[UVW]}$.

{hkl}	Spin direction [UVW]							
	[001]	[100]	[$\bar{1}$10]	[$\bar{1}$01]	[$\bar{1}\bar{1}$2]	[$\bar{1}\bar{1}$1]	[$\bar{1}\bar{1}$7]	Observed
{$\bar{3}$11}	91	54	35	82	98	86	97	Large
{11$\bar{3}$}	9	46	65	18	2	14	3	Small
{33$\bar{1}$}	47	27	46	27	20	7	39	Small
{$\bar{1}$33}	53	73	54	73	80	93	61	Large

[15] The calculations of Nagamiya and Matizuki were based on our original data, which do not differ significantly from the present values. Their work was presented at the Crystal Physics Conference, Massachusetts Institute of Technology, July, 1957.
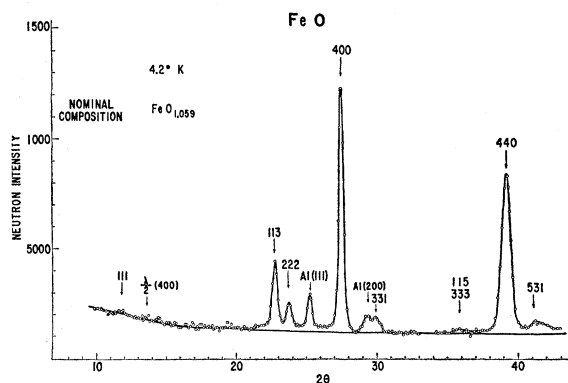
[16] N. Elliott, J. Chem. Phys. **22**, 1924 (1954).

TABLE VI. Neutron diffraction intensities for FeO at 77°K.

	Neutron intensities	
hkl	Calculated $A_{[111]}$	Observed[a]
111	0	20[b]
113	141	142
222	40	40
400	467	473
331	30	30
333	12	12
115		
440	478	478
531	29	41

[a] Cylindrical specimen 2-cm diam $f_{Fe} = 0.945 \times 0.96 \times 10^{-12}$ cm, $f_O = 0.58 \times 10^{-12}$ cm, $\bar{\mu}_{Av} = 3.32 \mu_B$; $2B = 1 \times 10^{-16}$ cm^2.
[b] Diffuse.

(111) planes and with spin directions alternately up and down with respect to the sheets.

A comparison of the intensities of the observed Bragg peaks and those computed confirm the assignment of structure $A_{[111]}$ for FeO (Table VI). The composition of the compound corresponded to the ratio Fe/O = 0.945 and neutron intensities were computed assuming vacancies randomly distributed among the iron sites and an average moment per site of $\mu = 3.32 \mu_B$.

DISCUSSION

The principal areas of uncertainty in deducing specific spin structures from the neutron scattering data relate to the proper magnetic scattering amplitudes and form factors required for the computation of the diffraction patterns from various assumed spin arrangements; questions about the neutron scattering process itself, which arise as a consequence of the observation of diffuse non-Bragg neutron intensity; and the uniqueness of a spin model which satisfies the neutron diffraction powder intensities.

Theoretical intensities computed for models of MnO should be reliable; the Mn^{+2} ion is in an S state, the magnetic form factor is isotropic, and magnetic scattering cross section depends on spin only. Although the Ni^{+2} ion is in an F state, the orbital contribution is largely quenched in the pseudocubic crystalline field and the isotropic spin-only scattering assumption should be a reasonable first approximation. The situation is different for Co^{+2} and Fe^{+2} and appreciable orbital contribution to the magnetic scattering may occur. In the present work we have used isotropic[17] form factors based on values calculated from Hartree-Fock radial functions,[18] which are in general agreement with $f_{Mn^{+2}}$ deduced by Corliss and Hastings.[19]

The quantitative agreement of the magnetic and nuclear scattering confirms the spin-only value of $5\mu_B$

for the moment of Mn^{+2}. Similarly, the moment of Ni^{+2} is approximately equal to the spin-only value of $2\mu_B$, although the relatively weak magnetic scattering from NiO (F_{mag}^2 is approximately 15% that of MnO) reduces the precision of the measurements. The magnetic scattering from CoO is much greater than can be accounted for by the pure spin moment of $3\mu_B$, and the present estimate $3.8\mu_B$ is to be compared with the value 4.2 deduced for Co^{+2} from paramagnetic susceptibility measurements on solid solutions of CoO in MgO, and $4.0\mu_B$ from the high-temperature suscepti-bility data of LaBlanchetais.[20]

The uniqueness of a solution of the spin structure deduced from neutron diffraction powder patterns must be discussed by recognizing the limitations imposed by the assumption that the elementary spins are parallel and antiparallel to an axis of magnetization in the unit cell. In a subsequent paper[21] the nature of the solution of the multimagnetic axis problem will be explored, and it is well to point out here that the consequent expansion of degrees of freedom leads to many diverse solutions compatible with the powder diffraction data. By limiting considerations to single-spin-axis solutions. the problem is reduced to discovering the nature of the antiferromagnetic coupling scheme around each magnetic ion and determining the direction of magnetization of the spins with respect to the crystal axes.

There are only two antiferromagnetic coupling schemes possible, A and B in Fig. 2. In both arrangements, each spin has six parallel and six antiparallel nearest neighbors, and six antiparallel next nearest neighbors. The neutron data clearly eliminate all spin structures based on the cubic coupling scheme B. Interpreting the diffuse neutron intensity as elastic spin scattering leads to a consistent set of solutions:

Salt	Structure	Magnetic axis
MnO	A	parallel to (111) plane
FeO	A	perpendicular to (111) plane
CoO	A	parallel to $[11\bar{7}]$ direction
NiO	A	parallel to (111) plane

These results suggest that for MnO and NiO the magnetic dipole-dipole interactions predominate and the choice of direction within the (111) plane is determined by second-order effects. Since the crystal distortion in the magnetically ordered state has rhombohedral symmetry, there is no angular dependence in the (111) plane of the deformation-produced anisotropy, and it is energetically easy to rotate the direction of magnetization as long as the spins lie within the sheet. As a result of the large exchange energy and small anisotropy constant, the thickness of the Bloch wall may be comparable to the domain dimensions,[22] and it is

[17] We have supplied our data to Professor T. Nagamiya who has carried out calculations for the neutron scattering based on the wave functions deduced by Kanamori for CoO. These results were reported at the Crystal Physics Conference, Massachusetts Institute of Technology, July, 1957.
[18] W. W. Piper (private communication).
[19] L. Corliss and J. M. Hastings (private communication).

[20] C. H. LaBlanchetais, J. phys. radium 12, 765 (1951).
[21] W. L. Roth (to be published).
[22] See, for example, C. Kittel, Introduction to Solid State Physics (John Wiley and Sons, Inc., New York, 1953), pp. 183–187.

reasonable to associate the diffuse neutron intensity with elastic scattering from the slightly disoriented spins which gradually change direction through the wall.

The crystallographic distortion of CoO has tetragonal symmetry and the anisotropy in the (111) plane is asymmetric. In agreement with this, the neutron diffraction data suggest a strong preference for a direction nearly parallel to the tetragonal axis. This suggests that the spin direction is a compromise between the dipole-dipole interactions which tend to hold the spins within (111) and the crystalline field energy arising from the deformation which favors a direction parallel to the tetragonal axis. In FeO the spin-orbit interactions apparently predominate, but since the crystallographic distortion is rhombohedral there is no conflict between the magnetic and crystalline anisotropies.

The alternative solution of the neutron diffraction data arrived at by considering only the sharp portion of the Bragg peaks is to maintain the spins coupled in a ferromagnetic sheet parallel to (111) but with the magnetic axis parallel to $[11\bar{1}]$. From symmetry considerations it seems unlikely that this is correct for MnO or NiO, although conceivably this result could be rationalized in the case of CoO as a consequence of the large spin-orbit interaction and crystalline deformation. A more likely explanation for the discrepancy in the intensity of the first magnetic peak is that the assumption of a common magnetic axis for all the magnetic moments is invalid, and in the case of CoO part of the discrepancy may be the consequence of an asymmetric magnetic form factor.

ACKNOWLEDGMENTS

Origin of Magnetic Anisotropy in Cobalt-Substituted Magnetite*

J. C. SLONCZEWSKI
International Business Machines Corporation Research Laboratory, Poughkeepsie, New York
(Received February 24, 1958)

The large part of the ferromagnetic anisotropy of $Co_xFe_{3-x}O_4$ attributed to the presence of Co^{2+} is explained, for small x, by means of a one-ion model. The residual orbital angular momentum $\alpha(\simeq 1)$ of Co^{2+} is constrained by the crystal electric field to lie parallel to the axis of trigonal symmetry. Spin-orbit energy $\lambda \mathbf{L} \cdot \mathbf{S}$ couples the spin to this axis, accounting for the anisotropy energy. By fitting the theory to cubic anisotropy data one finds $\alpha\lambda = -132$ cm^{-1}. The assumption that cations are mobile at higher temperatures leads to a quantitative explanation of the annealing-induced anisotropy energy. The mean orbital magnetic moment μ_L of Co^{2+} is predicted to be large ($\mu_L \simeq 0.5$ Bohr magneton) and anisotropic ($\Delta\mu_L \simeq 0.1$ Bohr magneton) at low temperatures.

1. INTRODUCTION

IT has been shown[1] by means of torque measurements on single crystals that the substitution of a small amount of cobalt for iron in magnetite ($Co_xFe_{3-x}O_4$) causes a large change in the magnetic anisotropy energy. The cubic anisotropy parameters K_1 and K_2 were found to depend strongly on temperature and, at a given temperature, to be approximately linear in x for $0 < x < 0.15$.

It has been found also that the anisotropy energy in cobalt-iron ferrites is affected by magnetic annealing.[2,3]

Suppose the temperature of the crystal is raised to an appropriate temperature T_a and the magnetization **M** is held for several minutes in a direction β by an applied magnetic field. If the crystal is then quenched to a temperature T, which is room temperature or lower, the free energy $\mathfrak{F}(T)$ is found to be a function of β as well as of the direction α of **M** at T. In general $\mathfrak{F}$ does not have cubic symmetry in α, although the crystal is cubic. Penoyer and Bickford[2] have investigated in detail the dependence of $\mathfrak{F}$ on α, β, and x for $0 < x < 0.15$.

It is the purpose of this paper to explain these effects. No attempt is made to explain the anisotropy energy of Fe_3O_4. Only the changes caused by substituting small amounts of cobalt are considered.

The basic assumption of the theory is that the lowest orbital level of Co^{2+} in the crystalline electric field is

* A brief description of this theory has appeared [J. Appl. Phys. **29**, 448 (1958)].
[1] Bickford, Brownlow, and Penoyer, Proc. Inst. Elec. Engrs. London **104B**, Suppl. No. 5, 238 (1957).
[2] R. F. Penoyer and L. R. Bickford, Jr., Phys. Rev. **108**, 271 (1957).
[3] Bozorth, Tilden, and Williams, Phys. Rev. **99**, 1788 (1955).